NASA/CR—1999-209150

Wide Temperature Characteristics of Transverse Magnetically Annealed Amorphous Tapes for High Frequency Aerospace Magnetics

Janis M. Niedra
Dynacs Engineering Company, Inc., Brook Park, Ohio

Prepared under Contract NAS3–98008

National Aeronautics and
Space Administration

Glenn Research Center

August 1999

Acknowledgments

This work was sponsored by the NASA Glenn Research Center under contract NAS3–98008, with G.E. Schwarze as the Project Manager.

Available from

NASA Center for Aerospace Information
7121 Standard Drive
Hanover, MD 21076
Price Code: A03

National Technical Information Service
5285 Port Royal Road
Springfield, VA 22100
Price Code: A03

Wide Temperature Characteristics of Transverse Magnetically Annealed Amorphous Tapes for High Frequency Aerospace Magnetics

Janis M. Niedra
Dynacs Engineering Company, Inc.
National Aeronautics and Space Administration
Glenn Research Center
Cleveland, Ohio 44135

Summary

100 kHz core loss and magnetization properties of sample transverse magnetically annealed, cobalt-based amorphous and iron-based nanocrystalline tape wound magnetic cores are presented over the temperature range of −150 to 150 °C, at selected values of B_{peak}. For B-fields not close to saturation, the core loss is not sensitive to temperature in this range and is as low as seen in the best MnZn power ferrites at their optimum temperatures. Frequency resolved characteristics are given over the range of 50 kHz to 1 MHz, at $B_{peak} = 0.1$ T and 50 °C only. A linear permeability model is used to interpret and present the magnetization characteristics and several figures of merit applicable to inductor materials are reviewed. This linear modeling shows that, due to their high permeabilities, these cores must be gapped in order to make up high Q or high current inductors. However, they should serve well, as is, for high frequency, anti ratcheting transformer applications.

Introduction

In most power converter and inverter circuits that utilize magnetic components, the inductors and transformers are a major contributor to mass and bulk. With internal operating frequencies of such aerospace power conditioners now being about 100 to 500 kHz, the magnetics losses nevertheless remain an order of magnitude below the total losses in the solid state switches and diodes. At this level, the magnetics losses detract less than 1 percent from an overall conversion efficiency that can reach 95 percent.

The concern to minimize losses at even the lowest levels arises from the multiplicative composition of the efficiencies of power processing blocks, chained in series and delivering a specified load power P_{load}. Thus the overall efficiency of a chain is $\varepsilon \equiv (\varepsilon_1 \cdot \varepsilon_2 \cdot \ldots \cdot \varepsilon_n)$ and generates a power loss of $(\varepsilon^{-1} - 1)P_{load}$. The loss power usually amounts to waste heat that adds to the size of the heat rejection apparatus in aerospace applications.

The loss contribution of any one processor depends on its location in the chain. The 'inefficiency' $\delta_i \equiv 1 - \varepsilon_i$ of the i^{th} processor from the start of the chain contributes

$$P_{loss,\,i} = P_{load}\,\delta_i / (\varepsilon_i \cdot \varepsilon_{i+1} \cdot \ldots \cdot \varepsilon_n) \tag{1}$$

to the losses, or input power. And its differential contribution is

$$dP_{loss,\,i} = \frac{P_{load}}{(\varepsilon_{i+1} \cdot \ldots \cdot \varepsilon_n)} \cdot \frac{d\delta_i}{\varepsilon_i^2} \ . \tag{2}$$

One can verify that

$$\sum_{i=1}^{n} P_{loss,i} = P_{load} \cdot (\varepsilon^{-1} - 1) \ , \tag{3}$$

as expected, and also note the special cases

$$P_{loss,1} = P_{load}\,\delta_1 / \varepsilon \tag{4}$$

and

$$dP_{loss,1} = P_{load}\,d\delta_1 / (\varepsilon\,\varepsilon_1) \ . \tag{5}$$

The overall efficiency ε will often be considerably less than unity, amplifying the effect of δ_1 the most.

And this consideration is further constrained by a consensus that 'progress' requires both system mass and individual building block, i.e., converter, mass to be minimized. A percent efficiency gain is significant and valuable in advanced power conditioners, whereas a device that adds mass to achieve this is hard to sell. Thus in the context of aerospace applications, a magnetic material that can maintain a lower core loss over the applicable temperature range can provide a basis for nosing out the competition.

Amorphous ribbons of certain metallic alloys, usually based on Co and/or Fe, are well known to exhibit extremely low core loss (refs. 1 and 2), that is as low as that of the best ferrites in the above frequency range and nowhere near as temperature sensitive. Moreover, their B-H characteristics can be controlled from highly square to linear by magnetic anneal and, in some cases, by partial recrystallization. Instability of magnetically interactive defects in the amorphous structure contributes to the very low coercivity. Near zero ($\lambda_s < 0.1\times10^{-6}$) saturation magnetostriction can be obtained in the Co-based ribbons. And these amorphous materials have a plastic yield strength 5 to 10 times that of say the competing crystalline Ni-Fe magnetic materials (Permalloys, 50%Ni-Fe), making the magnetic properties of the amorphous tapes insensitive to rough handling. It has been recognized now for over a decade that these amorphous ribbons or tapes represent an advanced technology permitting new solutions for high frequency aerospace magnetics.

Sample Cores

This work presents the core loss and magnetization properties of a few sample amorphous and partially recrystallized ('nanocrystalline') tape wound cores. Most of the data was taken at 100 kHz (sinusoidal) over the temperature range of ±150 °C, at selected peak B-fields (B_{peak}, or B_p). Core loss and magnetization data is also presented as a function of frequency, but only for $B_p = 0.1$ T at 50 °C. Although not exhaustive, this data is sufficient for an overview and some design decisions. It is also more detailed than what is available in the literature.

Unpackaged cores, listed in Table I, were obtained from Vacuumschmeltze GmbH. They are representative of commercially available, competitive types and are not intended to be a specific endorsement. These cores fit in a nominal size group specified by H = 0.25 in., ID = 1.00 in., and OD = 1.25 in., although their actual dimensions deviated slightly. Stated tape thickness for the 6025F and 500F materials was about 23 μm (0.91 mil) and about 17 μm (0.67 mil) for the 6030F material.

The 6025F is a Co-based, relatively low saturation induction (B_s), very low core loss, high permeability, transverse magnetically annealed type, intended for fast pulse transformers and common mode chokes. The 6030F is also a Co-based, low core loss, transverse magnetically annealed material, but with a lower permeability, a lower temperature sensitivity, better linearity and a higher B_s. The 6030F is intended for power and pulse transformers that require a low remanent induction. The 500F is a low core loss, Fe-based material of unspecified composition and anneal. Most likely it is an Fe-Si-B based, partially recrystallized metallic glass having a very fine grain structure of nanometer sized bcc Fe crystals throughout the bulk, that has been subjected to a transverse magnetic anneal. Its composition thus may be similar to that of the Hitachi Metals, Ltd. *Finemet* alloy ($Fe_{73.5}Cu_1Nb_3Si_{13.5}B_9$) (ref. 3), where the simultaneous presence of both Cu and Nb is known to enhance the soft magnetic properties of this optimally annealed, partially recrystallized amorphous, Fe-Si-B based alloy. Also, the possibility of extra surface recrystallization to induce a compressive stress magnetic anisotropy in the bulk, perpendicular to the surface of the ribbon, exists (ref. 4). According to the manufacturer, the 500F is a high permeability, flat B-H loop material, having extra thermal stability and intended for high frequency inductor, transformer and common mode choke applications. The λ_s is specified to be less than 0.2 ppm for the 6025F and 6030F materials, and less than 0.5 ppm for the 500F. However, no measurements of λ_s were made in this work.

Measurement Technique

Bare cores were placed in thin walled aluminum cases that were closed on top by an insulating washer. Cursory checks showed that the eddy current losses in these cases were negligible under the measurement conditions. This arrangement permits the cores to be tested over a wide temperature range without adverse effects from an encapsulant. However, an undamped core does permit the buildup of magnetostrictive resonances in cases where such could be significant.

Data consisting of waveforms of the current in a primary exciting winding and induced voltage in a secondary sense winding were recorded by a digitizing oscilloscope. The current sensor was a Pearson model 2877 current

transformer and the oscilloscope was a Tektronix model TDS 540. The secondary voltage was sensed differentially, simply by channel subtraction. The driving amplifier was a push-pull arrangement of two Apex model 19A high power operational amplifiers. At times a parallel tuning capacitor was used to relieve the amplifier from handling reactive current. With 3 well matched oscilloscope probes, in most cases this setup provided data accuracy better than 5 percent to at least 1 MHz and losses of the order of 1 part in 100 V/A product could be resolved. Depending on the frequency and B_{max}, either 5- or 10-turn windings were used. This type of measurement setup has been reported in a NASA soft magnetic materials evaluation program (ref. 5), as well as in published literature (ref. 6). A new variation was the use of a gated signal burst, either in a single shot or a repetitive averaging mode, to decrease the duty cycle. Core temperature then could be held accurately constant while measuring very high core losses.

Core Loss Characteristics

Temperature resolved specific core loss data at 100 kHz is presented for the 3 materials mentioned in figure 1. At the selected values of B_p, the curves naturally fall into triplet groups. At low temperatures, the lowest curve in each group is for the 6025F material, the next higher being for the 6030F and the highest being for the 500F. Magnetic saturation eliminates the 6025F from the $B_p = 0.7$, 1.0 T groups and the 1.0 T group has only the 500F.

Several observation are apparent from this data. First, the core loss is rather constant with temperature over a span of 300 °C, at least at the lower B_p, which is similar to the properties of low loss Ni-Fe crystalline materials, such as Supermalloy.

As the temperature increases, the core loss of a material can start to increase disproportionately. Presumably this is due to the onset of magnetic saturation and is very prominent in figure 1 for the 6025F, which has the lowest Curie temperature T_c as well as the lowest B_s. As B_p is increased, the effect becomes prominent also for the 6030F, which has the next higher T_c and B_s. Thus, as concerns losses, temperature effects can significantly influence, or even reorder, the relative ranking of these materials at values of B_p and temperature which are within tolerable limits. These limits are of course circumstantial. In previous NASA reports, a steady core loss exceeding about 1.7 W/cm^3 has been considered impractical, from the standpoint of heat removal. Long term operation of a 6025F core at 150 C would likely cause magnetic degradation, because magnetic anneals are usually performed at a temperature near T_c.

Finally, the 100 kHz core loss of these amorphous and partially amorphous materials is indeed low. For comparison to a lowest loss crystalline material, the 100 kHz core loss of 17 μm (0.67 mil) Supermalloy tape at 0.1 T is estimated to be 135 mW/cm^3. The only competition comes from certain low loss MnZn type ferrites, which can have comparably low losses: about 50 mW/cm^3 at 100 kHz and 0.1 T. However, the losses in ferrites are very temperature dependent and the 50 mW/cm^3 value only holds over a narrow temperature range.

Due to the limited scope of this experimental study, a frequency scan of the core loss was performed only at 50 C and a B_p of 0.10 T. Such data is of course valuable for broad band transformer applications and especially to evaluate the figures of merit of the material for resonant and filter inductor applications. Figure 2 shows the data obtained for the 3 materials to be the roughly straight lines usually seen for such log-log plots. Estimates of these core loss curves for other values of B_p can be made by a parallel shift of the curves in figure 2, based on the data versus at 100 kHz (fig. 1).

Using least squares fits to the data, the following estimates of $\overline{p}_c$ were obtained:

6025F: $\overline{p}_c = 2.44 B_p^{2.22} f^{1.76}$

6030F: $\overline{p}_c = 1.32 B_p^{2.08} f^{1.86}$

500F: $\overline{p}_c = 1.87 B_p^{2.09} f^{1.81}$.

Here $\overline{p}_c$ is in mW/cm^3, if B_p is in T and f in kHz. These estimates become poor for B_p approaching saturation.

Application to Inductive Elements

Amorphous and nanostructured magnetic ribbons are transverse magnetically annealed in order to linearize as much as possible their B-H characteristic and, moreover, to lower the permeability μ. This makes the materials useful to build inductors and flux ratcheting resistant, low remanence transformers for use in inverter circuits. When feasible,

this way of inducing a flattened, or sheared over, B-H characteristic is preferable to the complexity and often increased core loss associated with an air gap.

Review of Figures of Merit

A figure of merit defines what is important for an application and an inductor can have various specialized applications. Other than low core loss, such application specific figures of merit can disagree on the benefit of a specific core property. For example, high μ materials can reduce the core size for a given inductance L, but they are simply not suitable for high current inductors because of magnetic saturation. As μ is increased, the winding volume and resistive losses will be reduced, but the total Q of the inductor will eventually be pulled down by the reduced Q of the core. Here the complications of overall merits will be avoided by restricting to a few known measures of just the core material merit that can easily be computed from the presented data.

One frequently mentioned core material figure of merit is the μQ product, where Q refers to just the core material. appendix A shows that

$$\mu Q = \pi f B_p^2 / \bar{p}_c \ , \tag{6}$$

where $\bar{p}_c$ is the volume-specific core loss. Thus for a given f and B_p, this product is a measure of the reciprocal core loss. If the losses were classical eddy current, then $\bar{p}_c \propto f^2 B_p^2$ and $\mu Q \propto f^{-1}$.

Q itself is a measure of energy storage efficiency, and is computable from equation (6), once μ is known. Q can also be evaluated directly from the core loss waveform data, as indicated below, and equation (6) then gives μ. The reader should recall again that the above Q applies only to the core material and represents the high frequency region of the total Q of the inductor. At low frequencies, the winding losses start to dominate and cause the total Q to fall off.

$B_{max}/\mu^{1/2}$, or equivalently, the volume density $B_{max}^2/(2\mu)$ of stored energy, is a measure of the merit of a core material to make up an inductor of a specified L to absorb voltage spikes. Here B_{max} is the maximum useable B-field of the material, as set by linearity requirements. The basis for this quantity is the relation

$$\int_0^\tau |v(t)| dt = 4 B_{max} \ (L V_c / \mu)^{1/2} \ , \tag{7}$$

where v(t) is any applied voltage of period τ, zero average value, a single zero crossing internal to a period, and V_c is the core volume. This relation gives the volt time area handling capability of an inductor and is derived in appendix A. Its application requires caution, because the simple formula for L (eq. (A19)) shows that, for fixed V_c and L, the $N/\bar{\ell}_c$ will increase as μ decreases. A large number of turns per unit mean length of the core can cause problems. For example, an air core construction may require too thin a wire or have an unacceptably low Q.

Magnetization and Energy Storage Properties

Appendix A applies the usual parallel L-R circuit to model core loss and magnetization properties in the linear region of the dynamic B-H characteristic of the core. Winding losses would be represented by a resistance in series with the parallel L-R combination, but that is not relevant here because the voltage is effectively sensed across the L-R by means of a secondary sense winding that carries negligible current. It then becomes a simple task to assign a μ and a Q to the core via this L-R model. The Q is available from equation (A6) and the relative permeability μ_r from equation (A14), since the volt ampere product, $V_p I_p$, is here a part of the experimental data.

The μ_r for 100 kHz is plotted against temperature for the 3 materials in figures 3 to 5. As may be expected for a linear B-H characteristic, the μ_r of these materials is not very sensitive to B_p until saturation sets in. This is the interpretation suggested for the drooping with increasing temperature of some of the higher B_p curves. These plots also suggest that the 500F is qualitatively different from the other two materials. The temperature sensitivity of the μ_r for the 500F is of opposite sign and bigger.

The f dependence of the μ_r of the 3 materials is presented in figure 6, at 0.10 T and 50 C only. On a log-log scale, these plots seem to fit the shape of such plots seen in manufacturers' literature: a relatively flat low frequency region, going into rolloff as f increases and flattening again at high f. It is apparent too that a full illustration of this behavior

requires wider frequency data than was obtained. The insensitivity of the 6030F μ_r to f in the 50 kHz to 1 MHz range should be noted for resonant inductor applications.

The f dependence of the 3 core materials Q is presented in figure 7, but again only for 0.10 T at 50 C. Around and below 100 kHz, the curves drop rapidly with increasing frequency, reaching values less than unity in the case of the 500F and 6025F. Such surprisingly low values can be understood from the fact that the core Q is a composite of both magnetization and core loss properties, as both equations (6) and (A6) show. Even though the core loss is low, the μ_r is high and such that the $\mu_r \overline{P}_c$ product grows faster than f at constant B_p. Thus even below 100 kHz, all of these materials may need to be gapped to obtain a high Q.

For applications requiring volt-time area handling capability in an inductor of a given inductance and core volume, the 6030F has an advantage, according to equation (7), primarily because of its lower permeability.

Summary and Conclusions

100 kHz core loss and magnetization data was obtained over the temperature range of −150 to 150 °C for two amorphous and one partially recrystallized core materials. All of the selected materials have low magnetostriction ($\sim 0.2\times10^{-6}$) and a flat magnetization characteristic induced by transverse magnetic annealing. Each of these was picked to be representative of a class of commercial products:

1. A relatively low saturation (~0.5 T), cobalt based, amorphous tape, having very low losses and high permeability ($\sim 10^5$ at low frequency).
2. A higher saturation (~0.8 T), cobalt based, amorphous tape having low losses, a relatively low, but perhaps more stable, permeability ($\sim 3\times10^3$) and a higher Curie temperature.
3. A more recently developed, iron based, nanocrystalline tape, featuring some of the desirable soft magnetic properties of the cobalt based, amorphous tapes, but at a lower cost.

As expected from the manufacturer's literature, the core loss of these materials was indeed very low. At 100 kHz and 0.1 T, this loss was about 50 mW/cm^3, and relatively constant from −150 to 150 °C, for the amorphous 6025F material. This is as good as the best MnZn power ferrites can do at their optimum temperatures. Under these conditions, the highest loss seen was about 70 mW/cm^3, for the nanocrystalline 500F material. As long as operation was at low B-fields, the core loss was rather insensitive to temperature in the above range, for all 3 materials. At higher B_{peak}, above say 0.2 T, the significant increase in loss seen above a certain temperature may be attributed to onset of magnetic saturation, as the effect appeared to be ordered according to the Curie temperatures of these materials.

A frequency scan of the core loss of these materials showed the characteristics to be the usually seen, more or less straight lines on a log-log scale. This was done from 50 kHz to about 1 MHz, but only at 0.1 T and 50 C. The core loss frequency slope was somewhat less than for an f^2 dependence for all 3 of these materials, with the 6030F being the closest to f^2.

A parallel inductor-resistor circuit was used to model the linear magnetization properties of the 3 materials. This provides simple formulas that assign properties such as the relative permeability μ_r and 'quality factor' Q to the core material from the original exciting current and induced voltage data. The $\mu_r Q$ figure of merit is shown to be closely related to the reciprocal specific core loss.

At 50 C and $B_{peak} = 0.1$ T, the relative permeability measured in the frequency range of 50 kHz to 1 MHz for the three materials ranged from thousands to nearly 10^5. The permeability of the 6030F material was the lowest and least sensitive to frequency in the above range. Both of the cobalt based, amorphous materials (6025F, 6030F) exhibited a permeability increasing with temperature in the −150 to 150 C range, for low B-fields. In contrast, the permeability of the partially recrystallized, iron-based material (500F) decreased with temperature.

All three types of materials characterized here are suitable for very low loss, flux ratcheting resistant, high frequency power transformers, but they are not suitable to make up high Q inductors, unless cut and gapped to lower their permeability. Unfortunately, gapping a tape wound core often leads to a remarkably increased core loss, concentrated near the cut faces. H. Fukunaga et al. (ref. 7) have attributed the gap loss in cut, Co-based amorphous and Fe-based, recrystallized tape wound cores to in-plane eddy currents caused by the gap leakage B-field normal to the tape surfaces. And they have shown that in the case of such materials, the introduction of thin ferrite pole face plates can produce an inductor core superior to a gapped ferrite.

Appendix A

Linear Modeling of Core Magnetization Properties

A magnetic core whose material is describable by a linear relation $B = \mu H = \mu_r \mu_0 H$, at least for $|B| < B_s$, can be modeled by linear circuit elements. Note, however, that hysteresis losses can not be modeled accurately this way. A parallel combination of inductance L_c and resistance R_c will be used here to represent the core. Hence for sinusoidal excitation, the relation between the voltage (or its time integral) across the $L_c - R_c$ pair and the current into this pair is an ellipse. In the case of a time integrated voltage, this ellipse represents the apparent dynamic B-H hysteresis loop of the core. Any nonlinearity in the intrinsic B-H characteristic of the core material will be reflected as a distortion of the ellipse. Assuming negligible winding capacitance, the current measured in the exciting winding (N_1 turns) of a test core is the current into the $L_c - R_c$ pair. And the voltage across this $L_c - R_c$ pair is just (N_1/N_2) times the voltage sensed by a zero current secondary winding N_2.

Equivalent circuit Q

A general definition of the quality factor Q of an energy storing component is as 2π times the ratio of the peak stored energy to the energy dissipated per cycle. For an arbitrary impedance $\tilde{Z}$ (linear 2-terminal network), this can be shown to give

$$Q = \mathcal{Im}(\tilde{Z}) / \mathcal{Re}(\tilde{Z}) \tag{A1}$$

For an R_c in parallel with a reactance $X_c = \omega L_c$, one finds that

$$Q = R_c / X_c = R_c / (\omega L_c) \ . \tag{A2}$$

The magnitude I_p of the peak current into this is related to the magnitude V_p of the peak voltage across $\tilde{Z}_c$ by

$$I_p^2 = (V_p / R_c)^2 + (V_p / X_c)^2 \ . \tag{A3}$$

Noting that $V_p = \sqrt{2} V_{rms}$, and also recognizing that $V_{rms}^2 / R_c = \overline{P}_c$ is the total core loss, the relation (A3) can be rewritten into the form

$$(V_p I_p)^2 = 4(\overline{P}_c)^2 + (V_p^2 / X_c)^2 \tag{A4}$$

Division of equation (A4) by $(2\overline{P}_c)^2$ then gives

$$(R_c / X_c)^2 = \left(\frac{V_p I_p}{2 \overline{P}_c} \right)^2 - 1 \ , \tag{A5}$$

from which follows immediately that

$$Q = \left[\left(\frac{V_p I_p}{2 \overline{P}_c} \right)^2 - 1 \right]^{1/2} \tag{A6}$$

Equation (A6) determines the core Q in terms of the measured total core loss $\overline{P}_c$ and the peak voltage and current. One can also show by applying trigonometric identities to the explicit voltage-current product time function $v(t) \cdot i(t)$ that the $V_p I_p$ product is the same as the peak-to-peak value of $v(t) \cdot i(t)$:

$$V_p I_p = \left(v(t) \cdot i(t) \right)_{p-p} \ . \tag{A7}$$

This is useful to estimate the limits to Q measurement imposed by instrument resolution, since $\overline{P}_c = \overline{v(t) \cdot i(t)}$.

Formula for the μQ product

A quick way to arrive at a formula for μQ (or $\mu_r Q$) is to combine the basic peak induced voltage formula

$$V_p = N_1 \omega A_c B_p \tag{A8}$$

with the inductive reactance formula

$$X_c = \omega L_c = \omega \mu N_1^2 A_c / \overline{\ell}_c \tag{A9}$$

such as to get

$$V_p^2 / X_c = \omega V_c B_p^2 / \mu \ , \tag{A10}$$

where $V_c = \overline{\ell}_c A_c$ is the core volume. The V_p can be eliminated from equation (A10), since

$$V_p^2 = 2 R_c \overline{P}_c \tag{A11}$$

relates it to the average total core loss $\overline{P}_c$. Recalling equation (A2), this last step yields

$$Q = R_c / X_c = \omega B_p^2 / (2 \mu \overline{p}_c) \ , \tag{A12}$$

where $\overline{p}_c = \overline{P}_c / V_c$. The $\mu_r Q$ product then is

$$\mu_r Q = \pi f B_p^2 / (\mu_0 \overline{p}_c) \tag{A13}$$

Relative permeability μ_r of the core material

Equation (A13) is immediately useful to get μ_r, because Q is available from equation (A6). The result is

$$\mu_r \mu_0 = \omega B_p^2 / [(V_p I_p / V_c)^2 - 4 \overline{p}_c^2]^{1/2} \tag{A14}$$

Volt-time area handling capability

Let a periodic voltage v(t) impressed across an inductance L be such that $v(t) > 0$ for $0 < t < t_1$ and $v(t) < 0$ for $t_1 < t < \tau$, where τ is the period. Also, $\overline{v(t)} = 0$ is assumed. Since $\overline{v(t)} = 0$, the B(t) is periodic and may be assumed, without loss of generality, to swing between $-B_{max}$ and B_{max}, where $B_{max} > 0$. Integration of the magnetic induction law

$$v(t) = N \, d\phi/dt = N A_c \, dB/dt \tag{A15}$$

gives

$$\int_0^{t_1} v(t)\,dt = 2 N A_c B_{max} \tag{A16}$$

and

$$\int_{t_1}^{\tau} v(t)\,dt = -2 N A_c B_{max} \ . \tag{A17}$$

Noting the polarity of v(t), the above integrals can be combined in the form

$$\int_0^{\tau} |v(t)| dt = 4 N A_c B_{max} \quad . \tag{A18}$$

The number of turns N can be eliminated from equation (A18) by using the simple inductance formula

$$L = \mu N^2 A_c / \bar{\ell}_c \quad , \tag{A19}$$

which then puts equation (A18) into the final form

$$\int_0^{\tau} |v(t)| dt = 4 B_{max} \ (L V_c / \mu)^{1/2} \quad . \tag{A20}$$

References

1. Warlimont, H.: "The Impact of Amorphous Metals on the Field of Soft Magnetic Materials," Mater. Sci. and Eng., vol. 99, 1988, pp. 1–10.
2. Herzer, G. and Hilzinger, H.R.: "Recent Developments in Soft Magnetic Materials," Physica Scripta, vol. T24, 1988, pp. 22–28.
3. Yoshizawa, Y. and Yamauchi, K.: "Fe-Based Soft Magnetic Alloys Composed of Ultrafine Grain Structure," Materials Transactions, JIM, vol. 31, no. 4, April 1990, pp. 307–314.
4. Herzer, G. and Hilzinger, H.R.: "Surface Crystallization and Magnetic Properties in Amorphous Iron Rich Alloys," J. Magn. Magn. Mat., vol. 62, 1986, pp. 143–151.
5. Wieserman, W.R., et al.: "High Frequency, High Temperature Specific Core Loss and Dynamic B-H Hysteresis Loop Characteristics of Soft Magnetic Alloys," 25th Intersociety Energy Conversion Engineering Conference, Reno, NV, August 1990. Also NASA TM–103164.
6. Thottuvelil, V.J., et al.: "High-Frequency Measurement Techniques for Magnetic Cores," IEEE Power Electronics Specialists Conference, June 1985, pp. 412–425.
7. Fukunaga, H., et al.: "High Performance Cut Cores Prepared From Crystallized Fe-Based Amorphous Ribbon," IEEE Trans. Magn., vol. MAG-26, no. 5, September 1990, pp. 2008–2010.

Table I. Physical Properties of the Core Materials Characterized.

Type	Composition	B_s (T)	T_c (C)	T_x (C)	ρ ($\mu\Omega$m)	δ (g/cm^3)	λ_s (10^{-6})
6025F	$(CoFeMo)_{73}(SiB)_{27}$	0.55	210	540	1.35	7.70	< 0.2
6030F	$(CoFeMnMo)_{77}(SiB)_{23}$	0.80	350	480	1.30	7.75	< 0.2
500F	(?)	1.2	600		1.15	7.35	< 0.5

B_s - saturation magnetic induction
T_c - Curie temperature
T_x - recrystallization temperature
ρ - electrical resistivity
δ - density
λ_s - saturation magnetostriction

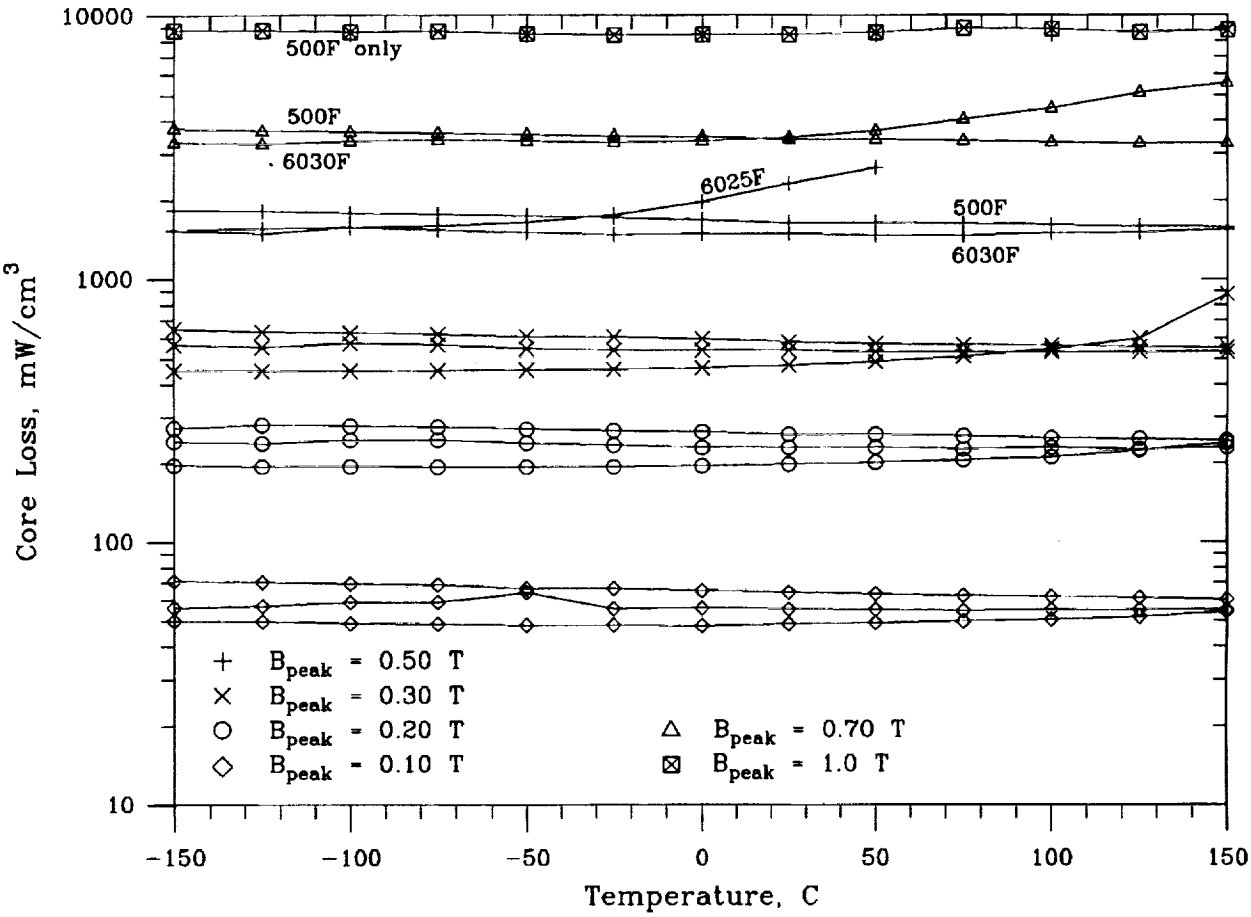

Figure 1.—Losses in amorphous tape-wound cores at selected peak flux densities. Excitation: 100 kHz sine wave. Materials in each B_{peak} group, in order of decreasing losses at low temperature: 500F, 6030F, 6025F.

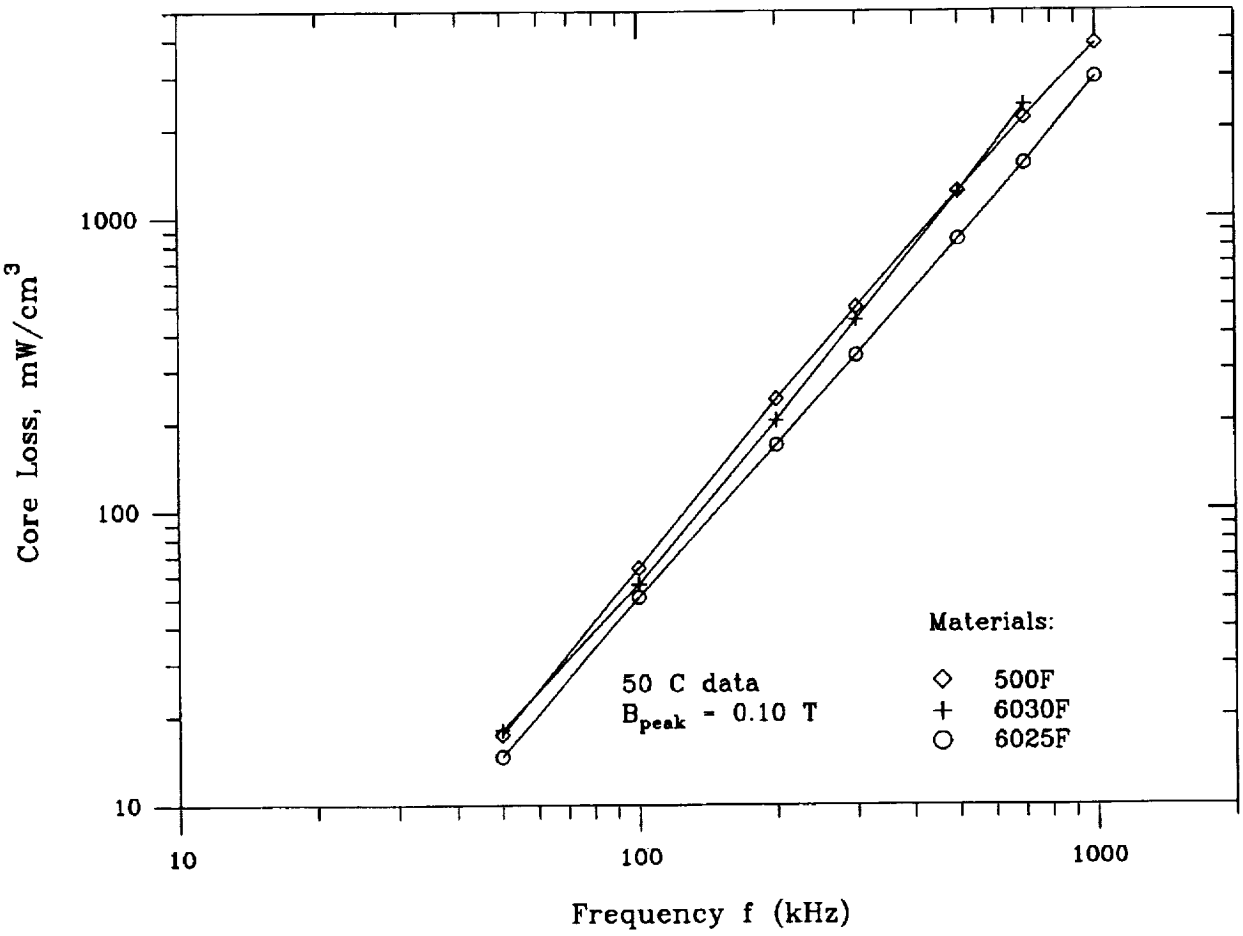

Figure 2.—Frequency dependence of the specific core loss of the 6025F, 6030F and 500F tape materials at 50 C and 0.1 T.

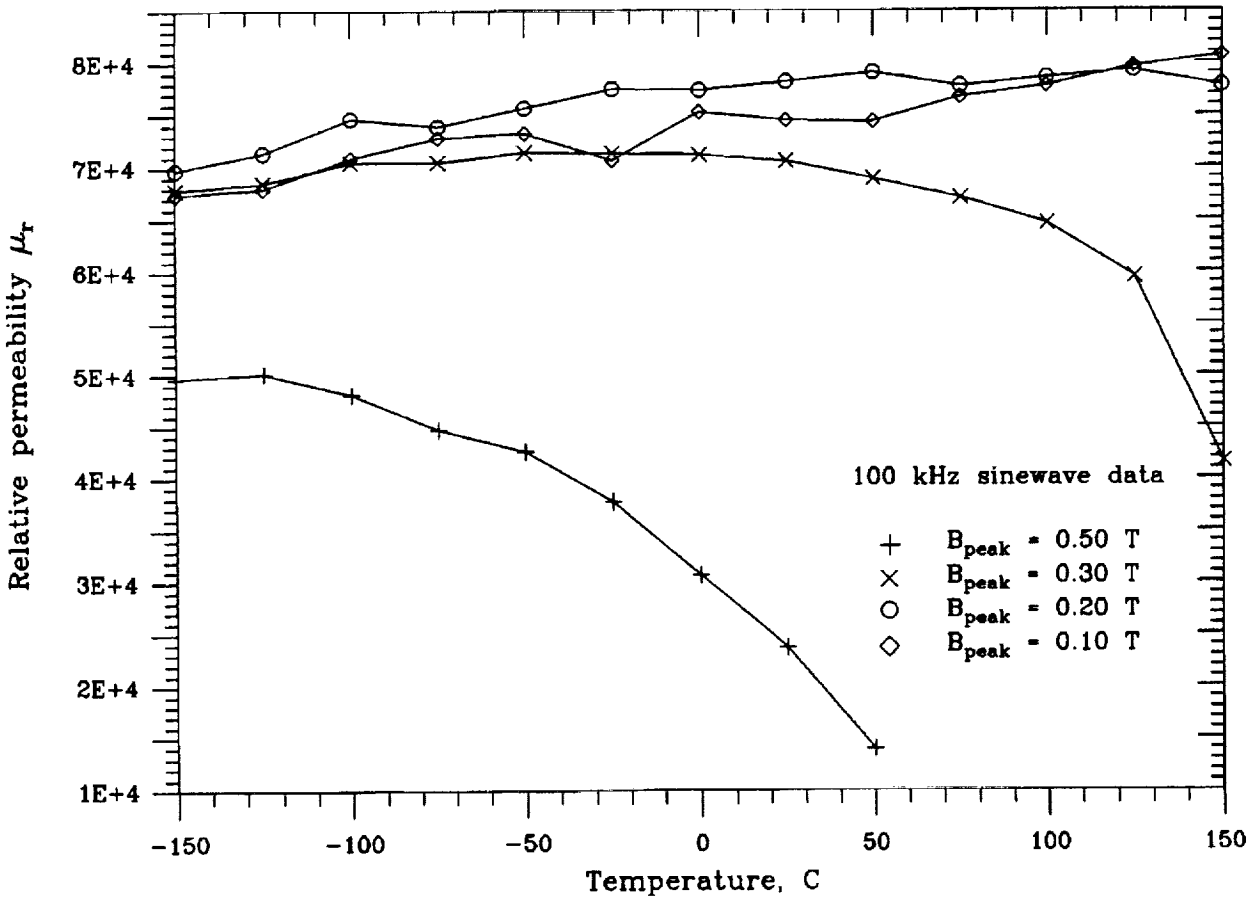

Figure 3.—Temperature dependence of the relative permeability of type 6025F amorphous tape at selected B_{peak} and f = 100 kHz.

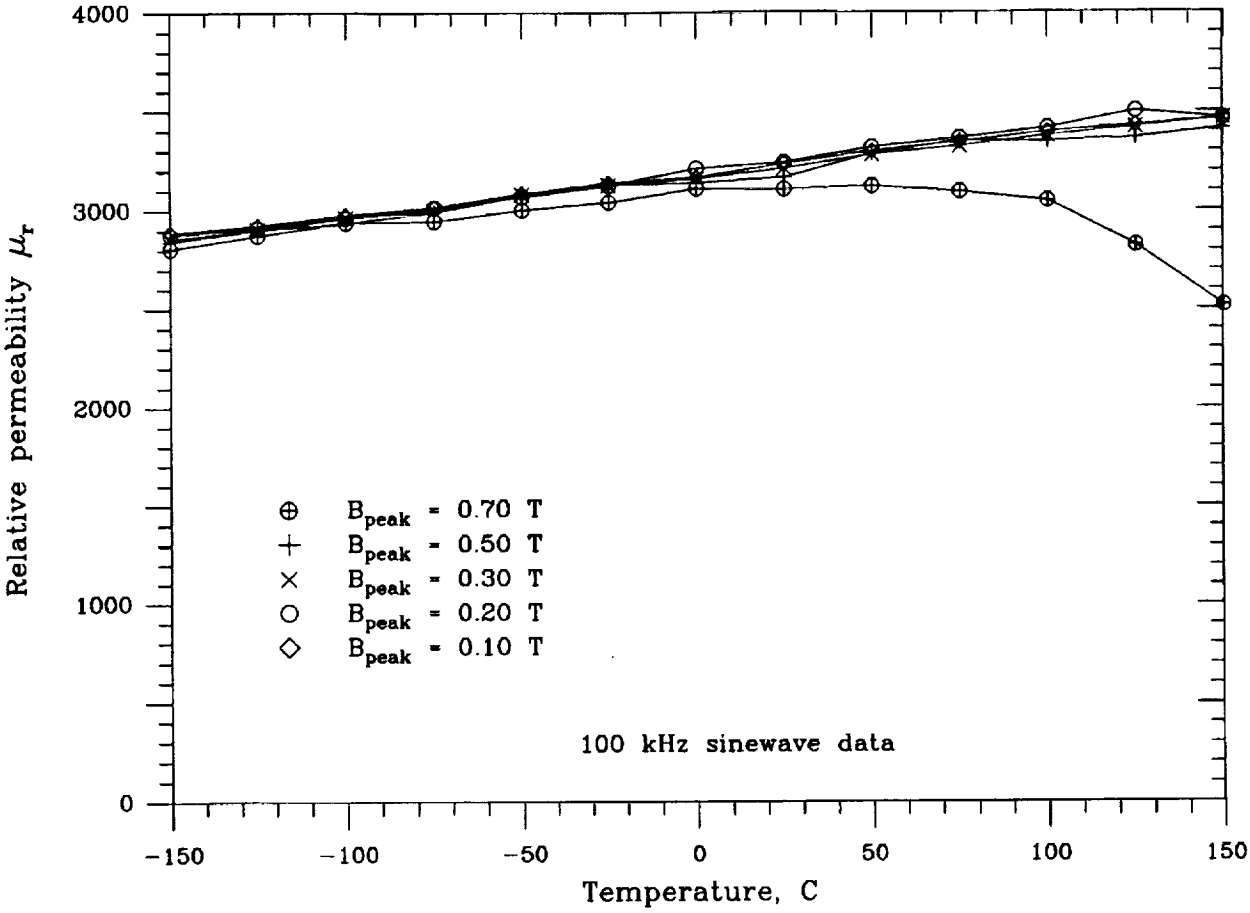

Figure 4.—Temperature dependence of the relative permeability of type 6030F amorphous tape at selected B_{peak} and f = 100 kHz.

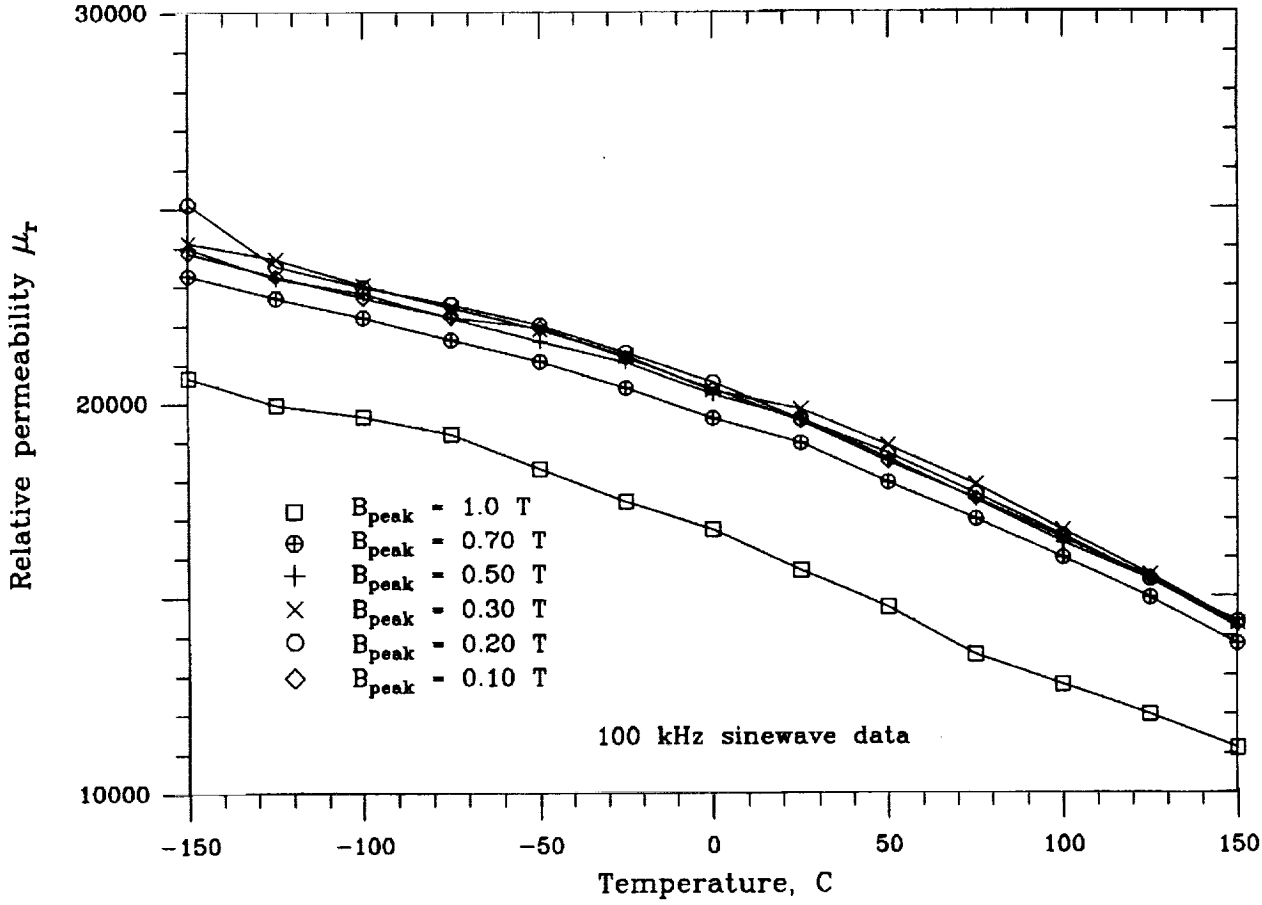

Figure 5.—Temperature dependence of the relative permeability of type 500F nanocrystalline tape at selected B_{peak} and f = 100 kHz.

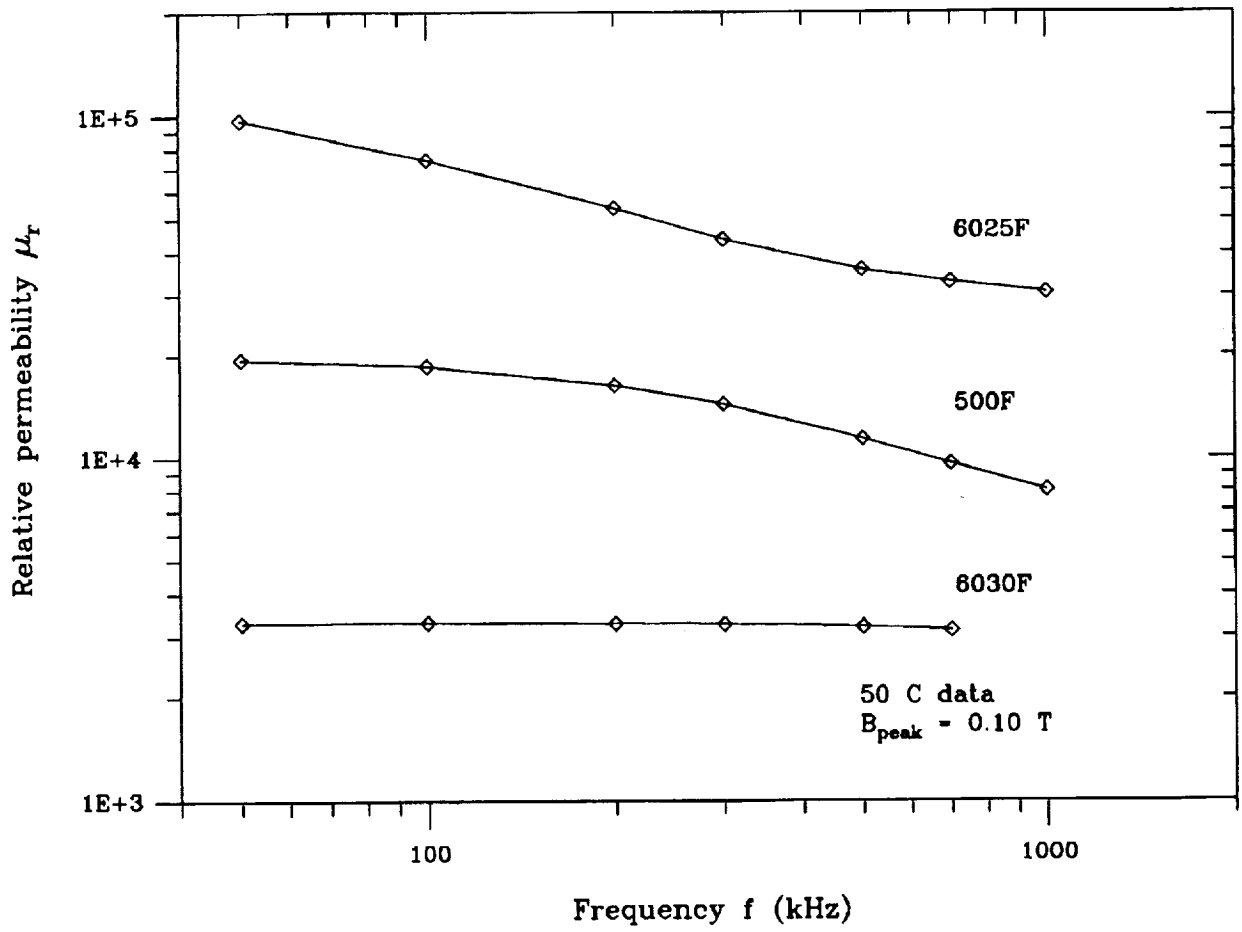

Figure 6.—Frequency dependence of the relative permeability of type 6025F, 6030F and 500F tape materials at 50 C and 0.1 T.

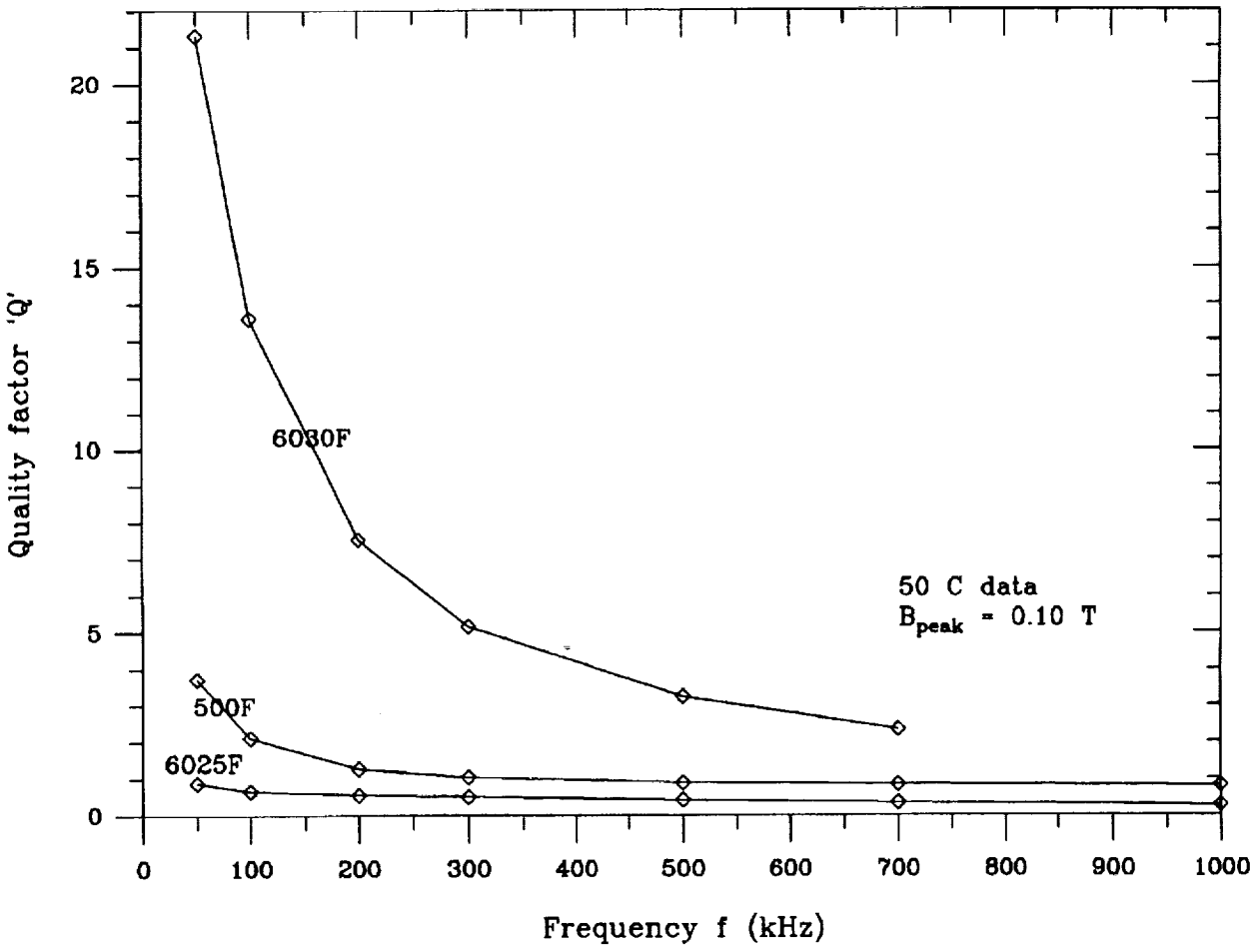

Figure 7.—Frequency dependence of the quality factor 'Q' of the 6025F, 6039F and 500F tape materials at 50 C and 0.1 T.

REPORT DOCUMENTATION PAGE

Form Approved
OMB No. 0704-0188

1. AGENCY USE ONLY (*Leave blank*)	2. REPORT DATE	3. REPORT TYPE AND DATES COVERED
	August 1999	Final Contractor Report

4. TITLE AND SUBTITLE

Wide Temperature Characteristics of Transverse Magnetically Annealed Amorphous Tapes for High Frequency Aerospace Magnetics

5. FUNDING NUMBERS

WU–632–1A–1C–90
NAS3–98008

6. AUTHOR(S)

Janis M. Niedra

7. PERFORMING ORGANIZATION NAME(S) AND ADDRESS(ES)

Dynacs Engineering Company, Inc.
2001 Aerospace Parkway
Brook Park, Ohio 441142

8. PERFORMING ORGANIZATION REPORT NUMBER

E–11637

9. SPONSORING/MONITORING AGENCY NAME(S) AND ADDRESS(ES)

National Aeronautics and Space Administration
John H. Glenn Research Center at Lewis Field
Cleveland, Ohio 44135–3191

10. SPONSORING/MONITORING AGENCY REPORT NUMBER

NASA CR—1999-209150

11. SUPPLEMENTARY NOTES

Project Manager, Gene E. Schwarze, Research and Technology Directorate, NASA Glenn Research Center, organization code 5450, (216) 433–6117.

12a. DISTRIBUTION/AVAILABILITY STATEMENT

Unclassified - Unlimited
Subject Category: 33 Distribution: Nonstandard

This publication is available from the NASA Center for AeroSpace Information, (301) 621–0390.

12b. DISTRIBUTION CODE

13. ABSTRACT (*Maximum 200 words*)

100 kHz core loss and magnetization properties of sample transverse magnetically annealed, cobalt-based amorphous and iron-based nanocrystalline tape wound magnetic cores are presented over the temperature range of –150 to 150 °C, at selected values of B_{peak}. For B-fields not close to saturation, the core loss is not sensitive to temperature in this range and is as low as seen in the best MnZn power ferrites at their optimum temperatures. Frequency resolved characteristics are given over the range of 50 kHz to 1 MHz, at B_{peak} = 0.1 T and 50 °C only. A linear permeability model is used to interpret and present the magnetization characteristics and several figures of merit applicable to inductor materials are reviewed. This linear modeling shows that, due to their high permeabilities, these cores must be gapped in order to make up high Q or high current inductors. However, they should serve well, as is, for high frequency, anti ratcheting transformer applications.

14. SUBJECT TERMS

Magnetic material; Power loss, Amorphous material, Wide temperature; High frequency

15. NUMBER OF PAGES
22

16. PRICE CODE
A03

17. SECURITY CLASSIFICATION OF REPORT	18. SECURITY CLASSIFICATION OF THIS PAGE	19. SECURITY CLASSIFICATION OF ABSTRACT	20. LIMITATION OF ABSTRACT
Unclassified	Unclassified	Unclassified	